Cell Genomics

Article

# Urine cf-nucleosomes: A non-invasive window into human physiology and disease

## Graphical abstract

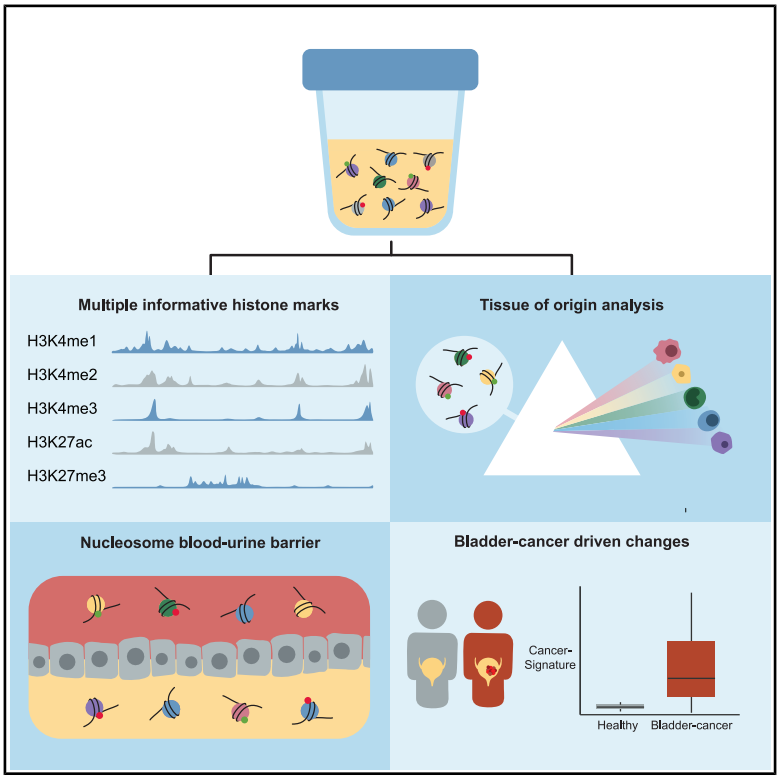


## Authors

Matan Lotem, Israa Sharkia, Batia Azria, ..., Hadar Rosen, Tal Falick-Michaeli, Nir Friedman

## Correspondence

nir.friedman@mail.huji.ac.il

## In brief

Using chromatin immunoprecipitation, Lotem et al. study post-translational modifications of cell-free chromatin fragments (cf-nucleosomes) shed by dying cells in the urinary tract. They identify the cellular origins of these fragments and how these cells change in disease. These results establish a new non-invasive window into human physiology and pathologies.

## Highlights

- Urine contains cell-free, post-translationally modified nucleosomes
- Bladder, kidney, and immune cells are the primary sources of urine cf-nucleosomes
- Blood cf-nucleosomes do not cross into the urine
- Urine cf-nucleosomes reflect bladder tumors and the immune response to the tumor

Lotem et al., 2025, Cell Genomics *5*, 100974
October 8, 2025 
https://doi.org/10.1016/j.xgen.2025.100974

CellPress

Cell Genomics

CellPress
OPEN ACCESS

Article

# Urine cf-nucleosomes: A non-invasive window into human physiology and disease

Matan Lotem,[1,2,3] Israa Sharkia,[1,2] Batia Azria,[4] Esther Harpenas,[1,2] Maayan Ormianer,[5] Hadar Rosen,[5] Tal Falick-Michaeli,[4,6] and Nir Friedman[1,2,3,7,*]

[1]The Lautenberg Center for Immunology and Cancer Research, Faculty of Medicine, the Hebrew University of Jerusalem, Jerusalem, Israel
[2]The Rachel and Selim Benin School of Computer Science and Engineering, the Hebrew University of Jerusalem, Jerusalem, Israel
[3]The Hebrew University Computational Medicine Center, the Hebrew University of Jerusalem, Jerusalem, Israel
[4]Department of Developmental Biology and Cancer Research Institute for Medical Research Israel-Canada, Hebrew University Medical School, the Hebrew University of Jerusalem, Jerusalem, Israel
[5]Department of Obstetrics and Gynecology, Hadassah Hebrew University Medical Center, Ein-Kerem, Jerusalem, Israel
[6]Department of Radiation and Medical Oncology, Sharett Institute of Oncology, Hadassah Hebrew University Medical Center, Jerusalem, Israel
[7]Lead contact
*Correspondence: nir.friedman@mail.huji.ac.il
https://doi.org/10.1016/j.xgen.2025.100974

## SUMMARY

Urine contains fragments of cell-free DNA (cfDNA) that offer molecular insights into processes within the urinary system and the body. It remains unclear whether these fragments exist as chromatin and retain chromatin modifications from their cells of origin. Here, we employ cell-free chromatin immunoprecipitation followed by sequencing (cfChIP-seq) on human urine to address this issue. We show that cf-nucleosomes can be captured from urine and preserve histone modifications associated with gene activation and repression. Analysis in healthy individuals reveals distinct tissue contributions to urine cf-nucleosomes, including a kidney-derived population not detected in matched exfoliated cells or plasma. This suggests that kidney filtration largely excludes plasma cf-nucleosomes. In patients with bladder cancer, urine cf-nucleosomes reflect tumor-associated transcriptional programs and immune responses. These findings highlight the utility of urine cf-nucleosomes as accessible, non-invasive biomarkers for studying renal physiology and monitoring urinary pathologies.

## INTRODUCTION

A long-standing goal in diagnostic medicine is to non-invasively monitor an individual's physiological status.[1] Non-invasive diagnostic tools are essential in the early stages of the diagnostic process when the clinician has to consider multiple hypotheses.[2] Blood and urine are two rich sources of information. Each collects molecules from large parts of the human body. Correspondingly, there is a wide range of blood and urine diagnostic tests for metabolites, proteins, nucleic acids, and more.[3]

Cell-free DNA (cfDNA) are fragments of DNA outside cells that circulate in bodily fluids, including urine. cfDNA from urine has proven to have diagnostic potential for various pathologies, including urogenital cancers such as prostate and bladder cancer[4] but also non-urogenital cancers such as glioma[5] and colorectal cancer.[6] Urinary cfDNA has also shown potential applications in monitoring urinary tract infections and organ transplant rejections[7,8] and in prenatal diagnosis.[9] Notably, urinary cfDNA can originate from healthy and diseased tissues, making it a valuable biomarker for assessing an individual's physiological and pathological states.[10]

Urinary cfDNA is reported to degrade within minutes to less than 3 hours by active DNase I in the urinary tract.[11–14] Thus, it originates from recent, close-to-urination time events. Urinary cfDNA originates from two sources. The first is from cells along the urogenital tract that shed DNA fragments through multiple pathways.[4] The second is from transrenal DNA fragments that pass from blood circulation, traversing kidney filtration.[15]

Some cell death pathways (e.g., apoptosis) result in the release of short chromatin fragments (complexes of DNA and proteins). The basic repeating units of chromatin are nucleosomes, each consisting of approximately 147 base pairs (bp) of DNA wrapped around a histone protein core composed of an octamer of histones H2A, H2B, H3, and H4.[16] During programmed cell death, DNases cut accessible linker regions between nucleosomes, and chromatin fragmentation displays a ladder of mono-, di-, and tri-nucleosome-length DNA fragments reflecting the underlying chromatin organization.[17]

Multiple lines of evidence show that most of the circulating cfDNA in the blood originates from fragments of nucleosome origin and that in the circulation, most of the cfDNA is still in intact complexes with histones.[18–23] Analogous questions arise in the context of urine cfDNA: is it of nucleosomal origin, and to what extent is it maintained as intact chromatin fragments? In particular, is transrenal cfDNA in the form of intact chromatin fragments?

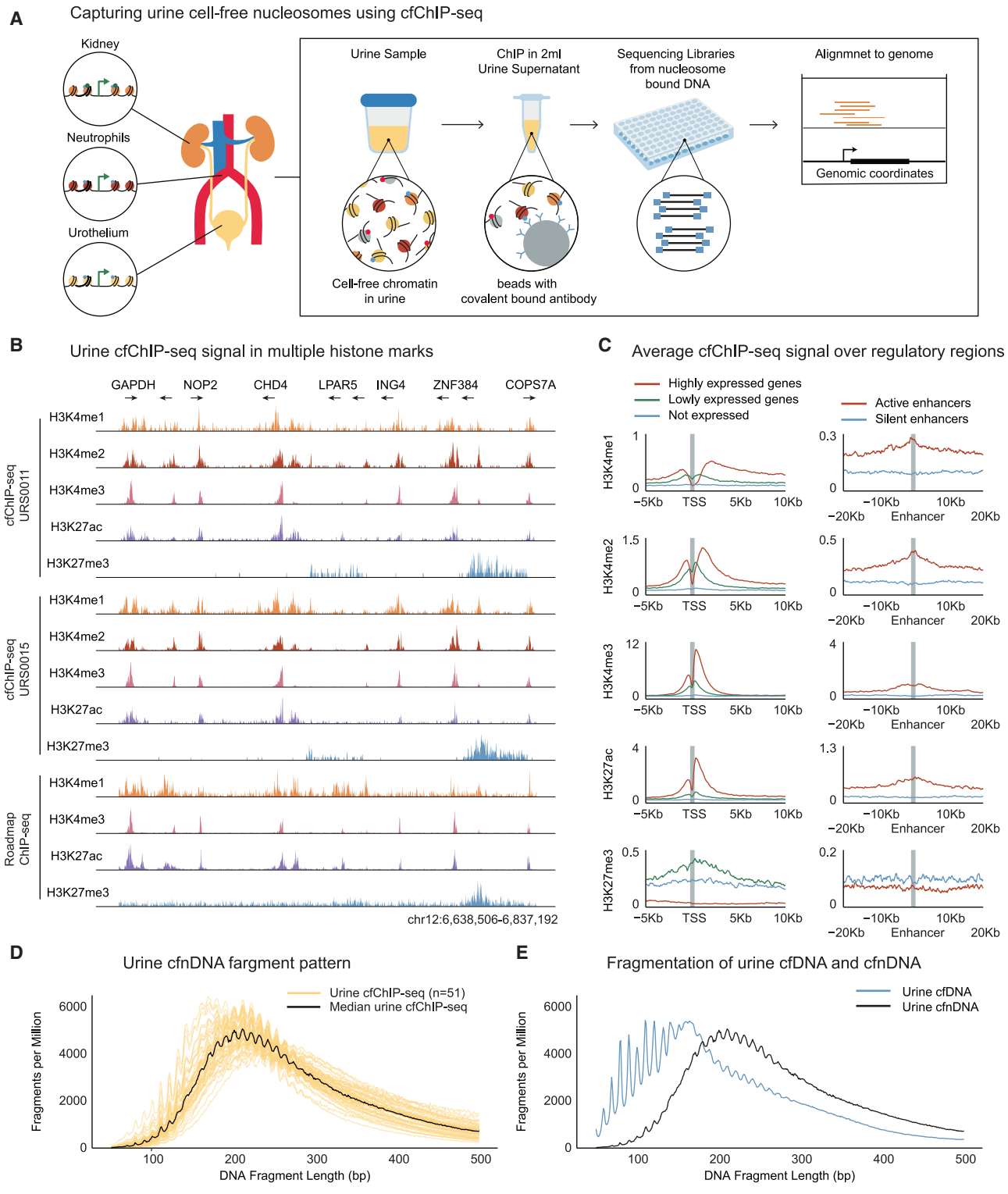


**Figure 1. cfChIP-seq of multiple histone modifications in human urine**

(A) Urine cfChIP-seq outline. Different cells release chromatin fragments into the urine. These fragments are immunoprecipitated using beads with covalently bound antibodies. DNA fragments are released, and sequencing libraries are generated.

(B) Genome browser view of histone modification signals. Three sets of tracks are shown: two from cfChIP-seq of healthy donors and one from published epithelial tissue ChIP-seq data.[49]

*(legend continued on next page)*

Histone proteins have been described in urine[24]; however, it is not known if they represent intact nucleosomes. Necrotic and apoptotic cells release chromatin into their immediate environment.[25] Thus, we expect to find cell-free nucleosomes (cf-nucleosomes) from dying cells of the urinary and genital tracts. Conversely, the process of urine formation by glomerular blood filtration ensures that large proteins with molecular weights >45 kDa rarely pass filtration.[26–28] Thus, a healthy kidney is expected to exclude plasma circulating nucleosomes (~179 kDa)[29] from the urine.

The harsh urine environment with active DNase digestion further complicates these questions. The length distribution of urine cfDNA suggests that most cfDNA fragments are partially digested,[11,14] in contrast to plasma cfDNA, which has characteristic peaks at mono- and di-nucleosome lengths (~170 and 320 bp).

In living cells, nucleosomes serve as a dynamic platform for DNA-associated processes. These processes involve chromatin-modifying enzymes that deposit and remove post-translational modifications of histones, such as methylation, phosphorylation, and acetylation, and chromatin-binding proteins that recognize specific modifications.[16] These chromatin modifications play central roles in transcription, replication, and DNA repair.[30–32] Histone marks offer clear and well-defined relationships to cellular processes, making chromatin analysis valuable for understanding cell identity and state.[33–35] For example, cardiomyocytes express the TNNT2 gene, and so only in this cell type would we encounter TNNT2-promoter nucleosomes marked with expression-associated marks[36] (e.g., acetylation, phosphorylation, tri-methylation, etc.). Some cancers, such as mixed lineage leukemia,[37] are characterized by epigenetic misregulation resulting in aberrant histone markings of oncogenes—indicative of a cancerous cell state.[38,39]

Recent works[40–42] show that many histone modifications survive in plasma cf-nucleosomes. By analyzing them, we recover rich information about gene activation, regulatory processes, and more. Capturing chromatin fragments with a specific modification (e.g., one associated with active promoters) and sequencing the associated DNA, we can identify genomic locations that had the modification in the cell of origin (e.g., active promoters in these cells) and learn about their identity and state.[42,43]

These results raise the question of whether urine nucleosomes, despite the harsh conditions, also carry cell-of-origin histone modifications and whether analyzing these can provide insights about their origin.

To answer these questions, we performed cell-free chromatin immunoprecipitation followed by sequencing (cfChIP-seq[42]) in human urine. We targeted both active (H3K4me1/2/3 and H3K27ac) and repressive (H3K27me3) histone marks and showed that urine contains cf-nucleosomes that retain multiple histone marks. Using cfChIP-seq against H3K4me3 (an active/poised promoter histone mark) in a cohort of healthy samples, we characterize the cell of origin of urine cf-nucleosomes. By comparing matched urine and plasma samples in healthy individuals as well as women pregnant with male fetuses, we show that negligible amounts of nucleosomes pass from plasma to urine, suggesting that urine and plasma are non-overlapping sources of epigenetic information.

To demonstrate the utility of examining cf-nucleosomes in urine, we considered monitoring of bladder cancer. This cancer originates from the urothelium, which lines the inner surface of the bladder. Bladder cancer is one of the most common cancers in humans, with more than half a million new cases worldwide and hundreds of thousands of subsequent deaths.[44] Bladder cancer affects ~4 times more men than women, and disease incidence increases with age.[44] Over 70% of patients diagnosed with bladder cancer are diagnosed with non-muscle invasive bladder cancer (NMIBC).[45] NMIBC has a high probability of recurrence and progression.[46] Currently, the gold standard in NMIBC monitoring is frequent cystoscopies,[47] which adversely affect the patients' quality of life.[48] Non-invasive approaches to monitoring and studying this cancer are an unmet need. cfChIP-seq profiles of a cohort of samples from patients with NMIBC highlight pathology-driven changes.

## RESULTS

### Modified circulating nucleosomes in human urine

We performed urine cfChIP-seq on urine samples from healthy individuals with antibodies targeting marks of accessible/active promoters (H3K4me3 $n$ = 51 and H3K27Ac $n$ = 7), enhancers (H3K4me2 $n$ = 13, H3K4me1 $n$ = 13, and H3K27Ac $n$ = 7), and repressive heterochromatin (H3K27me3 $n$ = 5) (STAR Methods; Figures 1A–1C). Assays were performed on 2 mL of urine supernatant, with pre-analytic assessment showing relative stability in 4°C for up to 2 weeks (STAR Methods). The resulting sequencing libraries yielded an average complexity of >13 million unique reads (STAR Methods) and an average of >80% alignment rates (Table S1). These quantities are consistent within an order of magnitude with total cfDNA concentrations in urine (Figure S1), suggesting that a non-trivial fraction of cfDNA is nucleosomal.

### Circulating nucleosome modifications originate from intact cells

Mapping the DNA sequences enriched in immunoprecipitated circulating nucleosomes to the genome, we observe stereotypical patterns in promoters and enhancers (Figures 1B, 1C, S2A, and S2B) for both active marks (H3K4me1/2/3 and H3K27ac) and repressive marks (H3K27me3). These patterns match the

(C) Metagene of normalized cfChIP-seq signal over promoters and enhancers. Line colors indicate activity levels of the genes based on >2,000 transcription start sites (TSSs) and enhancers from published ChIP-seq data.[50] The $y$ axis units denote coverage of fragments per million.
(D) cfChIP-seq DNA fragment size distribution. Thin yellow lines show DNA fragments from 51 urine cfChIP-seq samples of various histone modifications (H3K27ac $n$ = 6, H3K27me3 $n$ = 5, H3K4me1 $n$ = 13, H3K4me2 $n$ = 13, and H3K4me3 $n$ = 51), and the black line shows the median of all samples.
(E) Fragmentation patterns of urine ChIP-seq cfnDNA and urine cfDNA. The lines show the median of $n$ = 51 repeats in cfnDNA (black) and $n$ = 10 repeats in cfDNA (blue).
See also Figures S1 and S2.

profiles observed in tissue ChIP-seq (Figures 1B, 1C, and S2B). And as in tissue ChIP-seq, we observe H3K4me3 at promoters of active and poised genes, H3K4me2/1 at regulatory regions (promoters and enhancers), H3K27ac at active regulatory regions, and H3K27me3 surrounding repressed regulatory regions.

These results show that histone marks have the expected enrichment observed in intact cells. Given the high specificity of histone methyltransferase enzymes and their relatively low abundance in cells,[51] these marks are unlikely to be deposited after cell death, suggesting that histone modifications on circulating nucleosomes originate from intact cells.

## Circulating nucleosomes are a distinct subpopulation of cfDNA

ChIP enriches for histone-bound DNA, and thus, we will refer to the products of ChIP as cell-free nucleosomal DNA (cfnDNA). The lengths of cfnDNA fragments captured as a continuum in the range of mono-nucleosome (~170 bp) to tri-nucleosome (~400 bp) fragments (Figures 1D, 1E, S2C, and S2D). In contrast, urine cfDNA fragment lengths span a broader range from short (<100 bp) to long (>1,000 bp).[10,52] Specifically, the cfDNA pool includes many short fragments (<100 bp) that do not appear in the cfnDNA pool. This discrepancy is not due to technical sources (library preparation and sequencing protocols): we sequenced urine cfDNA using the same protocols used for cfChIP-seq (Figure 1E) and reproduced the same discrepancy in the short-fragment distribution. These results suggest that cfChIP-seq captures nucleosomal DNA fragments, which, by nature, are longer than 100 bp. In contrast, cfDNA sequencing captures an additional pool of non-nucleosomal fragments, including fragments shorter than 100 bp.

Both urine cfDNA and cfnDNA have a 10 bp length periodicity, consistent with DNase I digestion patterns (Figures 1E and S2D).[5,53,54] Together with the fragment length distribution, this suggests that the fragments recovered by ChIP-seq undergo multi-phase digestion, where nucleosomal ladder fragments (presumably digested at cell death) are subsequently digested in the urine by DNase I. This is consistent with the high abundance of DNase I in urine, which is also more active in urine than in plasma,[55,56] and the partial unwrapping of nucleosomes, mainly due to the high salt and urea concentrations in urine.[57]

## Tissues of origin of the urine cf-nucleosome pool

To further analyze the tissue origin of urine cf-nucleosomes, we focused on the H3K4me3 histone modification, which marks active or poised promoters and was shown to correlate with gene transcription and be informative of cell identity and state.[42] We used published ChIP-seq data to define tissue-specific signatures as promoters with a high signal only in one tissue type (STAR Methods; Figures 2A and 2B).

In nearly all healthy urine donor samples ($n$ = 56, Table S2), we observed a strong signal of urinary epithelium, kidney, and neutrophil signatures and, in a few samples, strong signals of macrophage, monocyte, B cell, and T cell signatures (Figure 2C). These signals are reproducible (technical repeats) and more similar in repeated samples from the same donor than in samples from different individuals (Figure S3A). We do not see contributions from other tissue types tested (Figures 2C and S3B). These are the expected cell types according to observations from cfDNA methylation in urine[11,58,59] and single-cell RNA sequencing (RNA-seq) of urine-exfoliated cells.[60,61]

Men and women differ genomically and anatomically, which is reflected in assay results. We did not observe sex differences in assay quality (Figure S3C). Yet, urine cfChIP-seq profiles differ between the sexes. Beyond the expected differences in sex chromosome read coverage (Figure 2D), a comparison of urine tissue signatures finds several sex-based differences (Figures 2D, S3D, and S3E). We observed significantly more urothelium in females compared to males. This is concordant with previous observations[61,62] and with increased cell exfoliation in the female urethra serving as a defense mechanism against pathogens.[63] We observed higher macrophage levels in females but did not observe significant sex-based differences in the levels of kidney and neutrophils.

## Urine cf-nucleosomes do not originate solely from exfoliated cells

Cells shed throughout the urinary tract reach the urine. These cells are potential sources for cfnDNA. Is it the only source? If so, we would expect the cell-type composition of cfnDNA to mimic the population of exfoliated cells. To test this hypothesis, we compared urine cf-nucleosomes to the chromatin of urine-exfoliated cells from the same individual (Figures 3A, 3B, S4A, and S4B) and systematically across multiple individuals (Figures 3C, S4C, and S4D).

As reported previously,[61,62] male urine contains negligible amounts of exfoliated cells, while female urine contains thousands to tens of thousands of exfoliated cells. Thus, our comparison focuses only on exfoliated cells from female subjects.

In both urine cfChIP-seq and exfoliated-cell ChIP-seq, we observe a significant signal associated with the epithelial signature. This aligns with previous findings that the majority of exfoliated cells in urine are of epithelial origin.[61,64] Consistent with earlier reports indicating that renal cells are rare in healthy urine samples,[61] we did not detect kidney-derived nucleosomes in exfoliated cells. However, we did detect kidney-derived nucleosomes in cfnDNA (Figures 3C and S4A). This suggests that, in healthy donors, most kidney-derived cfDNA arise from *in situ* cell death rather than exfoliation and subsequent cell death within the bladder. Stratifying the analysis by sex did not change these tissue distributions (Figures S4C and S4D).

## Glomerular filtration blocks plasma cf-nucleosomes from reaching the urine

In plasma, we observe megakaryocyte-derived and monocyte cfnDNA due to megakaryocyte cell death in the bone marrow and monocyte turnover in the circulation.[65,66] Despite a large contribution in all plasma samples, we do not observe megakaryocyte signatures in both urine fractions, suggesting that in healthy donors, these nucleosomes are effectively filtered in the kidney.

For a more definite test, we collected urine and plasma samples from six pregnant women, including matched and unmatched sample pairs, spanning gestational ages from 10 to 40 weeks. In 16 samples from 6 women carrying a male fetus,

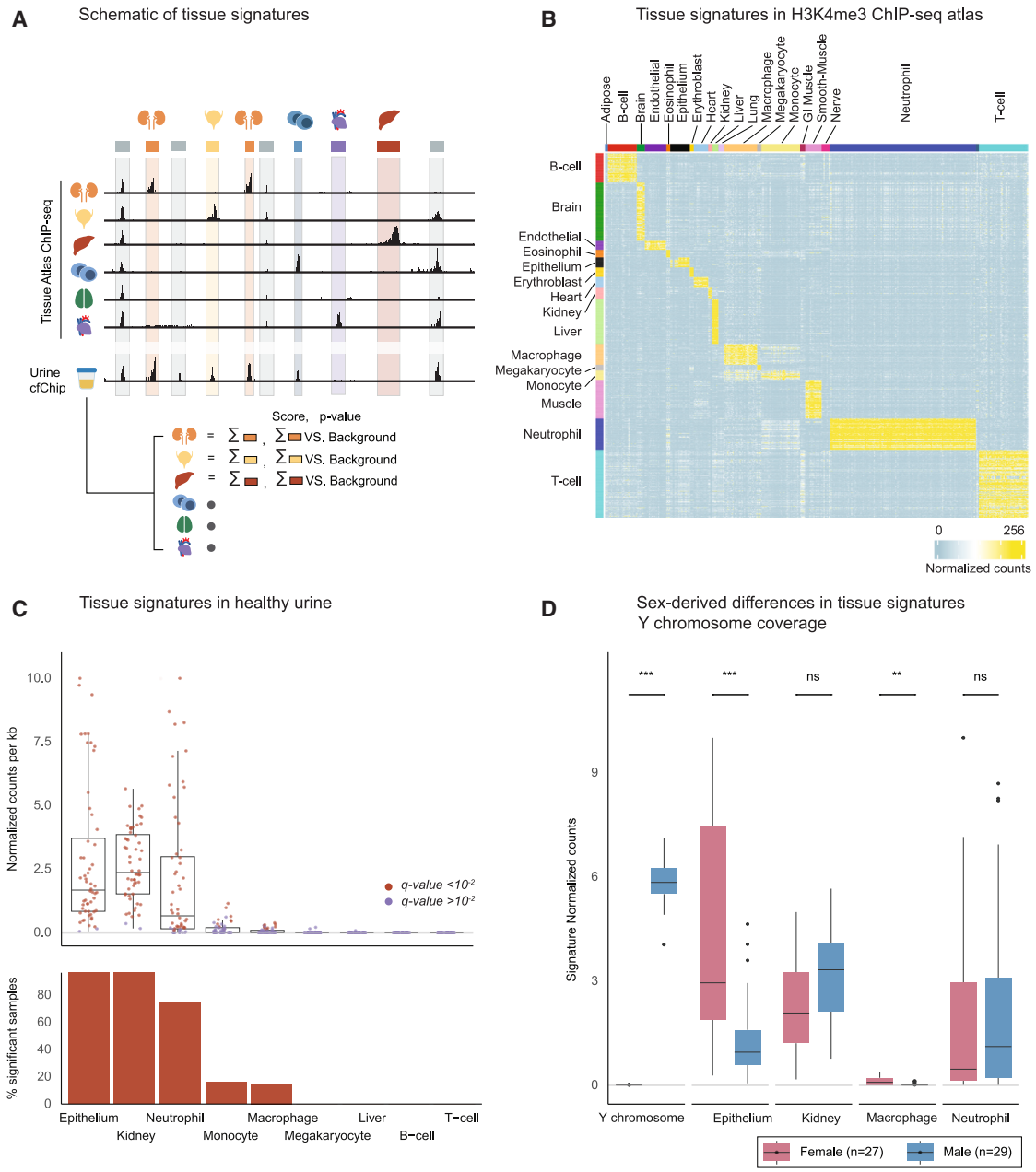


**Figure 2. cfChIP-seq detects cfnDNA cell of origin**

(A) Schematic of genomic regions used as tissue-specific signatures based on reference ChIP-seq tissue atlas. For each tissue (rows in genome browser view), we identify genomic locations with high signals only in the target cell type (column with colored matching icons; colored squares represent tissue-specific windows; gray windows are non-specific or background windows) Given a urine cfChIP-seq sample (bottom row and right side of illustration), we sum the signal at signature locations and test against the null hypothesis of non-specific background coverage (STAR Methods).

(B) Heatmap of tissue signatures (*y* axis) in H3K4me3 ChIP-seq signal of different tissues in the tissue atlas (*x* axis). Color indicates the normalized read count of each genomic window in each tissue.

(C) Top, tissue signatures in cfChIP-seq in 56 healthy samples from 21 donors. Each dot is a sample. Box limits: 25%–75% quantiles; the middle line indicates the median. The upper and lower whiskers extend to the largest and smallest values within 1.5× the interquartile range from the box edges. Dots in red indicate values significantly higher than background levels (STAR Methods). Bottom, percentage of samples with significant signals for each signature.

(D) Tissue signatures and Y chromosome coverage in female (27 samples from 9 donors) and male (29 samples from 12 donors) donors. Boxplots are as those described in (C). Wilcoxon test *p* values, adjusted for multiple comparisons, comparing the sexes are presented for each tissue signature: *adjusted $p < 0.05$, **adjusted $p < 0.01$, ***adjusted $p < 0.001$, and ****adjusted $p < 0.0001$. ns, not significantly different.

See also Figure S3.

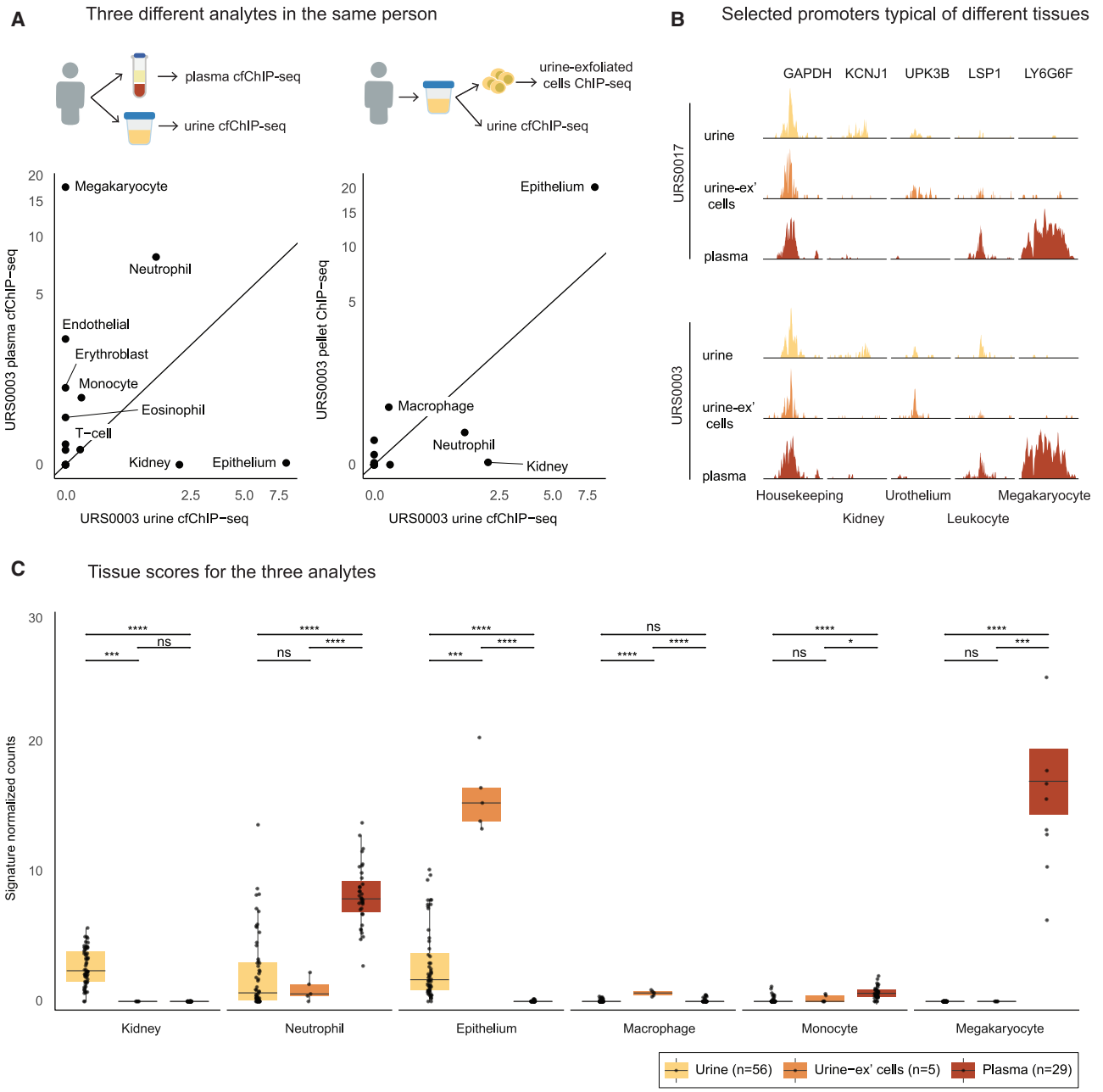


**Figure 3. Differences in promoter signals of three analytes**

(A) Comparison of urine cfChIP-seq (*x* axis) vs. donor matching plasma cfChIP-seq (*y* axis, left) and ChIP-seq of urine cells (*y* axis, right). Dots represent signature scores of labeled tissues.

(B) A genome browser view comparing the three analytes (urine cfChIP-seq, plasma cfChIP-seq, and urine-cell ChIP-seq) in two individuals. Each column features a promoter representative of a tissue type. Urine-ex' cells denote urine-exfoliated cells.

(C) Tissue signature distribution of multiple samples in the three analytes: urine cfChIP-seq (56 samples from 21 donors), urine cell ChIP-seq (5 samples from 4 donors), and plasma cfChIP-seq (35 samples from 35 donors). Each dot is a sample. Box limits: 25%–75% quantiles; the middle line indicates the median. The upper and lower whiskers extend to the largest and smallest values within 1.5× the interquartile range from the box edges. Wilcox-test adjusted *p* values for pairwise comparison between the three analytes are presented for each tissue signature: *adjusted $p < 0.05$, **adjusted $p < 0.01$, ***adjusted $p < 0.001$, and ***adjusted $p < 0.0001$. ns, not significantly different. Urine-ex' cells is shorthand for urine-exfoliated cells.

See also Figure S4.

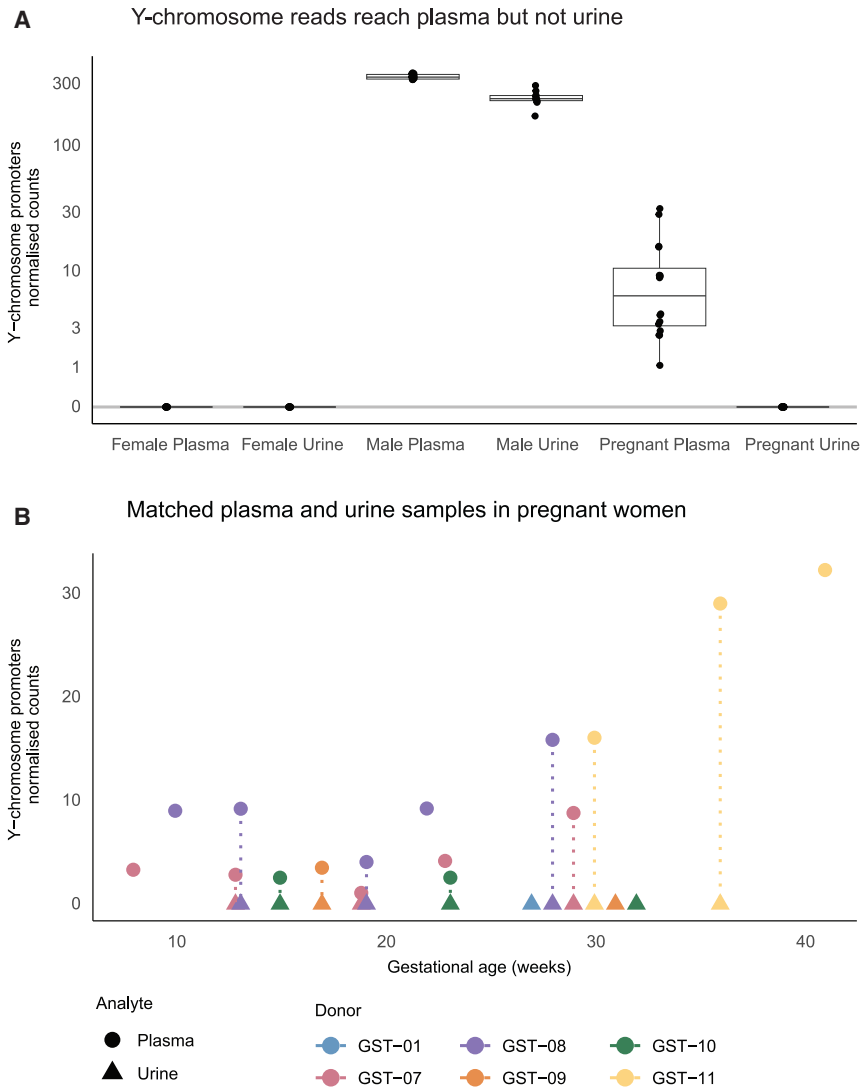


**Figure 4. Y chromosome cfChIP-seq signal in urine and plasma and in healthy and pregnant individuals**

(A) Normalized promoter coverage in the Y chromosome in urine and plasma samples from healthy non-pregnant females, males, and pregnant females with male fetuses.

(B) Normalized promoter coverage in the Y chromosome in urine and plasma samples from females pregnant with male fetuses across different gestational ages by week. Data point shapes represent sample type (dots are plasma cfChIP-seq samples, and triangles are urine cfChIP-seq samples), and colors indicate the pregnant donor. Plasma and urine samples from the same donor taken at the same gestational period are connected by dotted lines.

we observe reads from Y chromosome promoters in H3K4me3 from plasma (Figure 4A). However, we do not observe any reads from the Y chromosome in urine samples from the same women. We see an increase in the chromosome Y signal as gestational age increases in plasma but not in urine (Figure 4B). Previous results show that fetal cfDNA, in general and specifically from chromosome Y origins, can be captured in urine cfDNA.[9,67,68] Taken together, these results show that cf-nucleosome-bound cfDNA in the plasma does not reach the urine under healthy conditions.

## Urine in cell-free chromatin changes in patients with bladder cancer

To test the utility of urine cf-nucleosomes in differentiating between transcription patterns within the source tissue, we performed cfChIP-seq on urine samples from patients diagnosed with NMIBC (Table S2).

H3K4me3 urine cfChIP-seq performed on samples from 25 male patients with NMIBC showed hundreds of gene promoters with increased cfChIP-seq signals compared to a healthy reference (Figures 5A and S5A). To systematically evaluate these differences, we compared these NMIBC urine samples to urine samples from a cohort of 29 samples from 12 self-reported healthy males (Table S2). At the tissue-signature level, the NMIBC cohort samples show an increase in epithelium and immune cells compared to the healthy cohort (Figure S5B), presumably driven by the cancer's contribution to the cf-nucleosome pool. However, to better understand this contribution, we tested for differentially marked genes between the two cohorts and identified 177 genes with significantly elevated coverage and 61 genes with considerably decreased coverage (Figure 5B; STAR Methods), indicating changes in gene regulation between the groups.

In contrast to the significant differences in urine cfChIP-seq, no differences were found between the plasma cfChIP-seq results of healthy individuals and patients with NMIBC (Figures S4C and S4D), reiterating the value of urine as a valuable tool for the study and diagnosis of urinary system pathologies. To ensure these differences in signal are not due to the age differences between cohorts, we sampled three males aged over 70 without bladder cancer and observed little difference in gene signal (6 or fewer significantly increased promoters) compared to our healthy cohort. These promoters do not overlap with the signal we see in patients with cancer (Figure S5E).

## Changes in cfnDNA of patients with NMIBC are driven by cancer-related processes

Within the 177 genes with a significantly increased signal in the NMIBC cohort, we observe several bladder cancer expression biomarkers (e.g., KRT20,[69] GRHL3[70] FXYD3,[71] CA9,[72] and

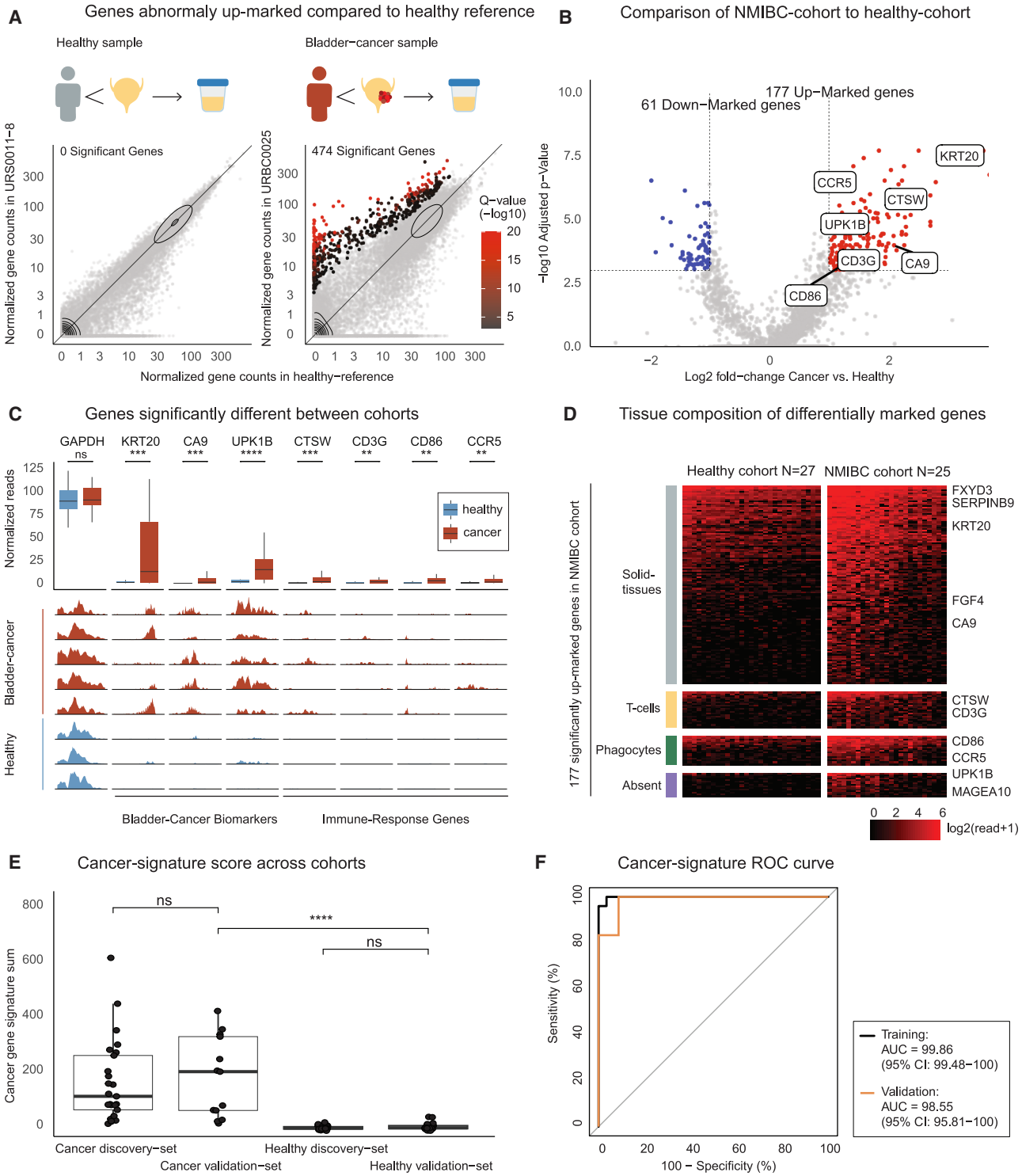


**Figure 5. Pathology-driven changes in NMIBC cohort**

(A) Detection of genes with significantly high coverage in a sample from a healthy urine sample (left) and the urine of a patient with NMIBC (right). For each gene, we compared mean normalized coverage in a reference healthy cohort (STAR Methods, *x* axis) against the normalized coverage in the cfChIP-seq sample (*y* axis). Significance tests whether the observed number of reads is significantly higher than expected based on the distribution of values in healthy samples (STAR Methods).

(B) Cohort comparison across genes. Statistical significance (*y* axis) and fold change of the NMIBC group over the healthy group (*x* axis) of genes in both groups. Significance values represent the false discovery rate (FDR)-corrected *q* value of the likelihood ratio test between two groups (STAR Methods).

*(legend continued on next page)*

UPK1B[73]), indicating oncogenic misregulation at the epigenomic level, observable using urine cfnDNA.

To further investigate the underlying tissue sources of these promoters in NMIBC samples, we used a reference H3K4me3 ChIP-seq cell-type atlas (STAR Methods; Figure 5D). We identified many of these up-marked genes as enriched in T cells (22/177 genes, EnrichR[74] ARCHS4 tissues[75] $q < 10^{-12}$) and phagocytes (19/177 genes, EnrichR ARCHS4 tissues $q < 10^{-16}$). These genes have a diminished signal in healthy urine cfChIP-seq and indicate a differential immune-cell state, presumably as a response to the tumor. Additional genes with increased signals were categorized as having signals in multiple solid tissues (122/177, solid tissue). Several increased-signal genes had absent signal levels in the reference atlas (15/177, absent), suggesting aberrant activation of pathways normally repressed in healthy adults (e.g., UPK1B[73] and MAGEA10[76]). Down-marked genes are enriched in the kidney (EnrichR ARCHS4 tissues $q < 10^{-8}$), in agreement with lower levels of kidney observed in cancer samples (Figure S5B).

To test if these observations generalize to unobserved urine samples, we defined a cancer signature utilizing gene promoters with a signal in cancer urines but unmarked in healthy urines (43 genes, termed the NMIBC signature; Table S3). This signature performs well in identifying the urine of patients with NMIBC when tested against a validation cohort of 23 healthy urine samples and 12 NMIBC urine samples withheld from analysis (Figures 5E and 5F; area under the receiver operating characteristic [ROC] curve [AUC] = 0.97; STAR Methods), indicating consistency in abnormal cancer-derived cfnDNA. The cancer signature levels correlate with cancer grade (Figure S6A). In contrast, the epithelial signature, reflecting bladder contribution, is not significantly different from cancer grade (Figure S6B).

## DISCUSSION

In this study, we investigated the presence and characteristics of cf-nucleosomes in urine. Using cfChIP-seq, we demonstrated that urine contains non-trivial quantities of intact nucleosomes carrying various histone marks, including H3K4me1, H3K4me2, H3K4me3, H3K27ac, and H3K27me3. Genomic alignment of the cfnDNA is consistent with the expected regions of the accompanying histone mark, suggesting that these histone marks are preserved from their cells of origin.

### Tissue sources of cfnDNA

Focusing on the H3K4me3 promoter mark, we delineated tissue contributions to urinary cf-nucleosomes, identifying diverse cell types, including bladder epithelial cells, kidney cells, and leukocytes. This group of originating cells agrees with prior studies with single-cell RNA-seq and DNA methylation profiling.[11,58–61]

Our observations of sex-based differences in cf-nucleosome profiles further enrich the growing literature on sex-based variability in cfDNA. The enriched population of epithelial cells captured in female samples could account for the increased levels of cfDNA described in female urine.[77]

When considering the differences between the cf-nucleosome populations in urine and plasma, our results strongly suggest that in healthy donors, plasma cf-nucleosomes rarely reach the urine. Megakaryocytes contribute much of the observed contribution to cfDNA in plasma[42,65] and are not observed in urine cf-nucleosomes, while kidney cf-nucleosomes are absent in plasma cf-nucleosomes. Additionally, the presence of plasma cf-nucleosomes originating from the Y chromosome in mothers of male fetuses, coupled with their absence in urine, strongly supports this conclusion. This barrier can be breached in various kidney pathologies,[78] which, we believe, can be analyzed using cfChIP-seq to expand upon these observations.

### Urine cfDNA fragmentation and origin

The observed cfnDNA fragmentation pattern in urine displays characteristics consistent with digestion patterns observed in plasma (nucleosomal ladder) and in cfDNA in urine (10 bp oscillations), suggesting a two-phase digestion mechanism—initial cleavage during cell death, followed by further digestion within the urine.[10–12] We show evidence that suggests that plasma circulating cf-nucleosomes do not traverse into urine under healthy conditions. In contrast, evidence of transrenal cfDNA[79] suggests that unbound plasma circulating cfDNA may pass to the urine. These findings suggest two different sources of cfDNA in urine and the distinction between nucleosomal cfDNA (recent cell death in the urinary tract) and non-nucleosomal cfDNA (either degradation of cfnDNA or transrenal cfDNA). This contrasts with plasma cfDNA, where chromatin dominates the circulating cfDNA pool, either as short fragments or longer ones.[18–20,23,80,81] Taken together, these results suggest that the possibly small amount of non-nucleosomal cfDNA fragments not removed by other mechanisms, such as liver uptake,[82] are efficiently removed from the plasma through glomerular filtration (Figure 6).

### Application in pathophysiology

Beyond cell-type variability, we used urine cf-nucleosomes to detect differences in cell states. In the urine of patients with NMIBC, we observed increased signals of bladder cancer

(C) Top, normalized count distribution of representative genes significantly different between the two cohorts. Red boxes represent NMIBC cohort samples, and gray boxes represent healthy samples. Box limits: 25%–75% quantiles; the middle line indicates the median. The upper and lower whiskers extend to the largest and smallest values within 1.5× the interquartile range from the box edges. Adjusted $p$ values from the Wilcoxon test for pairwise comparisons between the two cohorts are shown for each tissue signature: *adjusted $p < 0.05$, **adjusted $p < 0.01$, ***adjusted $p < 0.001$, and ****adjusted $p < 0.0001$. ns, not significantly different. Bottom, a gene browser view of representative genes significantly different between the two cohorts (red tracks are NMIBC cohort samples, and gray tracks are healthy samples).
(D) Heatmap representation of 177 genes significantly higher in the NMIBC cohort than in the healthy cohort. Rows (genes) are clustered by cell-type category. Heatmap values (colors) are log-transformed normalized values (log2 (1 + normalized gene reads)).
(E) Comparison of cancer signature levels across the healthy and NMIBC discovery cohorts and the validation cohorts. Boxplot description and statistical test are as described in (C).
(F) The receiver operating characteristic (ROC) curve illustrates the performance of a classifier using the cancer signature by plotting the true positive rate (sensitivity) on the $y$ axis against the false positive rate (1-specificity) on the $x$ axis.
See also Figures S5 and S6.

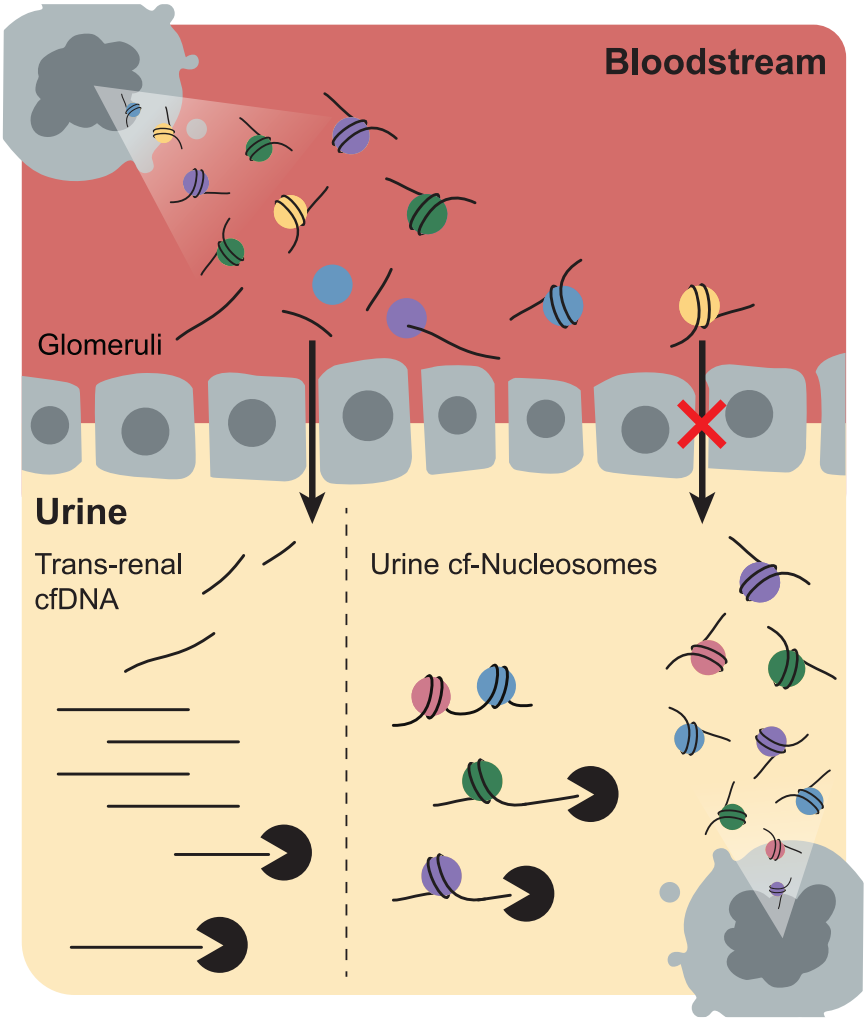


**Figure 6. Model of source of urine cfDNA**

Dying cells release cf-nucleosomes in the bloodstream that cannot traverse glomerular filtration into urine, as opposed to unbound cfDNA, termed transrenal cfDNA, after passage into urine. Transrenal cfDNA is rapidly digested in urine due to hyperactive DNase I. Cells and tissues with direct contact to urine (e.g., kidney, bladder epithelium, and some immune cells) contribute modified cf-nucleosomes to urine after cell death, which are also rapidly digested similarly to transrenal cfDNA and contribute to the general urine cfDNA pool.

expression markers and genes indicative of an immune response. Within the cancer signature (Table S2), we found many genes involved in the immune response (e.g., KLRK1, ICOS, and CTSW),[83] as well as previously described bladder cancer-associated genes (e.g., KRT14[84] and HYAL4[85]). These results align with the pathophysiology of bladder cancer, highlighting the utility of urine cf-nucleosomes in interrogating disease processes in the urinary tract.

## Advantages of profiling cf-nucleosomes

The use of cf-nucleosomes differs from existing urine liquid biopsy approaches in the following characteristics: (1) in contrast to targeted approaches (specific protein or metabolite, specific mutations, or enrichment to a panel of locations), we use genome-wide measurements, which are disease agnostic. The assay does not rely on predetermined markers or regions and can detect multiple facets of the patient's physiology. (2) Unlike DNA methylation, which is mainly lineage determined,[86] histone marks are dynamic and reflect the transcriptional/regulatory state of the cells that contribute to the cf-nucleosome pool.[42] (3) The connections to gene regulation allow exploitation of abundant information about gene expression in disease within the assay analysis (e.g., tumor sub-typing). (4) In contrast to fragmentomics approaches that examine coverage and fragment patterns at different genomic locations to infer the regulatory state,[87] which often require multiple genomic loci or very deep sequencing, histone marks provide direct, well-understood relationships to cellular processes and are informative about individual promoters. As such, the results are easier to interpret and are more robust to experimental and collection variability.

## Further research

Some open questions remain regarding urine circulating cf-nucleosomes: unlike plasma, urine is not homeostatically maintained, making it a highly variable environment. External factors like exercise, nutrition, postprandial sample collection, liquid intake, and the female menstrual cycle could affect results in a manner unexplored here. Additionally, this study collected all samples from individuals with self-reported properly functioning kidneys. Several kidney disorders are characterized by increased glomerular permeability (proteinuria),[78] which could lead to plasma cf-nucleosomes leaking into urine. Finally, while the H3K4me3 promoter mark is effective in cell-type and -state annotations, additional information can be obtained using additional histone marks, such as H3K27ac for the annotation of active enhancers and H3K36me3 for active transcription. We have only explored a small subset of the diverse histone marks, with many more holding information on other cellular processes.

## Conclusion

This study positions urinary cf-nucleosomes as a potent tool for studying human physiology and disease. By situating these findings within the broader landscape of cfDNA and epigenetic research, we demonstrate the unique advantages of these analytes in studying localized and systemic processes. Histone

marks' dynamic and tissue-specific insights promise to advance basic research and clinical applications, paving the way for more precise and comprehensive biomarker discovery.

### Limitations of the study

Here, we provide an exploration of the potential information in cf-nucleosomes in urine. In particular, we focused on ideal sample collection and handling (e.g., 4°C storage). These conditions are challenging to preserve in clinical settings. Thus, widespread use of such an assay would require technological solutions in the field of urine sample collection and storage, similar to the development of blood collection tools for cfDNA, which have advanced in recent years.[88]

Our analysis of NMIBC patient samples is preliminary. Moreover, the healthy population we compare against is not age matched. This is far from ideal and might over-amplify differences between cohorts. That said, the differences between low- and high-grade samples (age balanced) suggest that the cancer signature reflects the disease and not the subjects' age. These results are sufficiently promising to justify further exploration of the potential utility in larger, more diverse cohorts. Longitudinal studies of cf-nucleosomes from urine as the disease progresses can further connect these findings to larger disease contexts, such as disease recurrence, progression, and treatment efficacy.

## RESOURCE AVAILABILITY

### Lead contact

Further information and requests for resources and reagents should be directed to and will be fulfilled by the lead contact, Prof. Nir Friedman (nir.friedman@mail.huji.ac.il).

### Materials availability

This study did not generate new unique reagents.

### Data and code availability

- All datasets used in this study are available in the Zenodo repository: https://doi.org/10.5281/zenodo.15227938.
- All script files used in this manuscript's analysis will be available upon request. R code for processing cfChIP-seq data is available at https://github.com/nirfriedman/cfChIP-seq.git, and setup files for analysis are available in the Zenodo repository: https://doi.org/10.5281/zenodo.3967253.

## ACKNOWLEDGMENTS

We thank Oliver Rando, Eithan Galun, Tommy Kaplan, Ronen Sadeh, and the members of the Friedman lab for discussions and comments on this manuscript. We thank Lior Friedman for help with the illustrations and graphic design. This work was supported by the European Research Council's AdG Grant cfChIP 101019560 (to N.F.) and Israel Science Foundation IPMP Grant 3751/21 (to N.F.).

## AUTHOR CONTRIBUTIONS

Conceptualization, M.L., I.S., and N.F.; methodology, M.L. and I.S.; sample acquisition, B.A., E.H., M.O., and H.R.; investigation, M.L.; visualization, M.L.; funding acquisition, N.F.; project administration, M.L., I.S., T.F.-M., and N.F.; supervision, N.F. and T.F.-M.; writing – original draft, M.L.; writing – review & editing, M.L., I.S., B.A., T.F.-M., and N.F.

## DECLARATION OF INTERESTS

N.F. and I.S. are co-founders, shareholders, and serve on the management of Senseera, Ltd. N.F. is a co-inventor on a patent on using cfChIP-seq to diagnose diseases from body fluids.

## STAR★METHODS

Detailed methods are provided in the online version of this paper and include the following:

- KEY RESOURCES TABLE
- EXPERIMENTAL MODEL AND STUDY PARTICIPANT DETAILS
  - Donors
- METHOD DETAILS
  - Sample collection
  - H3K4me3 ChIP-seq of urine-exfoliated cells
  - Urine cfDNA extraction
  - Immunoprecipitation, NGS library preparation, and sequencing
  - Sequencing analysis
  - Epigenomics atlas
  - Tissue signatures
  - Tissue sources of cancer upregulated genes
  - Cancer-signature
- QUANTIFICATION AND STATISTICAL ANALYSIS
  - Comparison to background
  - Comparison to healthy reference
  - Comparison of two groups of samples
  - ROC analysis based on cancer signature scores

## SUPPLEMENTAL INFORMATION

Supplemental information can be found online at https://doi.org/10.1016/j.xgen.2025.100974.

Received: January 15, 2025
Revised: April 16, 2025
Accepted: July 21, 2025
Published: August 14, 2025

## REFERENCES

1. Zakari, S., Niels, N.K., Olagunju, G.V., Nnaji, P.C., Ogunniyi, O., Tebamifor, M., Israel, E.N., Atawodi, S.E., and Ogunlana, O.O. (2024). Emerging biomarkers for non-invasive diagnosis and treatment of cancer: a systematic review. Front. Oncol. *14*, 1405267. https://doi.org/10.3389/fonc.2024.1405267.
2. Brush, J.E., Jr., Sherbino, J., and Norman, G.R. (2017). How Expert Clinicians Intuitively Recognize a Medical Diagnosis. Am. J. Med. *130*, 629–634. https://doi.org/10.1016/j.amjmed.2017.01.045.
3. Zhang, Z., Liu, J., Cheng, Y., Chen, J., Zhao, H., and Ren, X. (2022). Urine Analysis has a Very Broad Prospect in the Future. Front. Anal. Sci. *1*, 812301. https://doi.org/10.3389/frans.2021.812301.
4. Lu, T., and Li, J. (2017). Clinical applications of urinary cell-free DNA in cancer: current insights and promising future. Am. J. Cancer Res. *7*, 2318–2332.
5. Mouliere, F., Smith, C.G., Heider, K., Su, J., van der Pol, Y., Thompson, M., Morris, J., Wan, J.C.M., Chandrananda, D., Hadfield, J., et al. (2021). Fragmentation patterns and personalized sequencing of cell-free DNA in urine and plasma of glioma patients. EMBO Mol. Med. *13*, e12881. https://doi.org/10.15252/emmm.202012881.
6. Su, Y.-H., Wang, M., Brenner, D.E., Norton, P.A., and Block, T.M. (2008). Detection of Mutated K-*ras*DNA in Urine, Plasma, and Serum of Patients with Colorectal Carcinoma or Adenomatous Polyps. Ann N.Y. Acad. Sci. *1137*, 197–206. https://doi.org/10.1196/annals.1448.027.

7. Zhang, J., Tong, K.L., Li, P.K., Chan, A.Y., Yeung, C.K., Pang, C.C., Wong, T.Y., Lee, K.C., and Lo, Y.M. (1999). Presence of donor- and recipient-derived DNA in cell-free urine samples of renal transplantation recipients: urinary DNA chimerism. Clin. Chem. *45*, 1741–1746.

8. Burnham, P., Dadhania, D., Heyang, M., Chen, F., Westblade, L.F., Suthanthiran, M., Lee, J.R., and De Vlaminck, I. (2018). Urinary cell-free DNA is a versatile analyte for monitoring infections of the urinary tract. Nat. Commun. *9*, 2412. https://doi.org/10.1038/s41467-018-04745-0.

9. Tsui, N.B.Y., Jiang, P., Chow, K.C.K., Su, X., Leung, T.Y., Sun, H., Chan, K.C.A., Chiu, R.W.K., and Lo, Y.M.D. (2012). High resolution size analysis of fetal DNA in the urine of pregnant women by paired-end massively parallel sequencing. PLoS One *7*, e48319. https://doi.org/10.1371/journal.pone.0048319.

10. Bryzgunova, O.E., and Laktionov, P.P. (2015). Extracellular Nucleic Acids in Urine: Sources, Structure, Diagnostic Potential. Acta Naturae *7*, 48–54.

11. Cheng, T.H.T., Jiang, P., Tam, J.C.W., Sun, X., Lee, W.-S., Yu, S.C.Y., Teoh, J.Y.C., Chiu, P.K.F., Ng, C.-F., Chow, K.-M., et al. (2017). Genome-wide bisulfite sequencing reveals the origin and time-dependent fragmentation of urinary cfDNA. Clin. Biochem. *50*, 496–501. https://doi.org/10.1016/j.clinbiochem.2017.02.017.

12. Yao, W., Mei, C., Nan, X., and Hui, L. (2016). Evaluation and comparison of in vitro degradation kinetics of DNA in serum, urine and saliva: A qualitative study. Gene *590*, 142–148. https://doi.org/10.1016/j.gene.2016.06.033.

13. Ruppert, T., Roth, A., Kollmeier, J., Mairinger, T., and Frost, N. (2023). Cell-free DNA extraction from urine of lung cancer patients and healthy individuals: Evaluation of a simple method using sample volume up-scaling. J. Clin. Lab. Anal. *37*, e24984. https://doi.org/10.1002/jcla.24984.

14. Augustus, E., Van Casteren, K., Sorber, L., van Dam, P., Roeyen, G., Peeters, M., Vorsters, A., Wouters, A., Raskin, J., Rolfo, C., et al. (2020). The art of obtaining a high yield of cell-free DNA from urine. PLoS One *15*, e0231058. https://doi.org/10.1371/journal.pone.0231058.

15. Umansky, S.R., and Tomei, L.D. (2006). Transrenal DNA testing: progress and perspectives. Expert Rev. Mol. Diagn. *6*, 153–163. https://doi.org/10.1586/14737159.6.2.153.

16. Kornberg, R.D., and Lorch, Y. (1999). Twenty-Five Years of the Nucleosome, Fundamental Particle of the Eukaryote Chromosome. Cell *98*, 285–294. https://doi.org/10.1016/s0092-8674(00)81958-3.

17. Kressel, M., and Groscurth, P. (1994). Distinction of apoptotic and necrotic cell death by in situ labelling of fragmented DNA. Cell Tissue Res. *278*, 549–556. https://doi.org/10.1007/BF00331373.

18. Snyder, M.W., Kircher, M., Hill, A.J., Daza, R.M., and Shendure, J. (2016). Cell-free DNA Comprises an In Vivo Nucleosome Footprint that Informs Its Tissues-Of-Origin. Cell *164*, 57–68. https://doi.org/10.1016/j.cell.2015.11.050.

19. Jiang, P., Chan, C.W.M., Chan, K.C.A., Cheng, S.H., Wong, J., Wong, V.W.-S., Wong, G.L.H., Chan, S.L., Mok, T.S.K., Chan, H.L.Y., et al. (2015). Lengthening and shortening of plasma DNA in hepatocellular carcinoma patients. Proc. Natl. Acad. Sci. USA *112*, E1317–E1325. https://doi.org/10.1073/pnas.1500076112.

20. Lo, Y.M.D., Chan, K.C.A., Sun, H., Chen, E.Z., Jiang, P., Lun, F.M.F., Zheng, Y.W., Leung, T.Y., Lau, T.K., Cantor, C.R., and Chiu, R.W.K. (2010). Maternal plasma DNA sequencing reveals the genome-wide genetic and mutational profile of the fetus. Sci. Transl. Med. *2*, 61ra91. https://doi.org/10.1126/scitranslmed.3001720.

21. Ivanov, M., Baranova, A., Butler, T., Spellman, P., and Mileyko, V. (2015). Non-random fragmentation patterns in circulating cell-free DNA reflect epigenetic regulation. BMC Genom. *16*, S1. https://doi.org/10.1186/1471-2164-16-S13-S1.

22. Chandrananda, D., Thorne, N.P., and Bahlo, M. (2015). High-resolution characterization of sequence signatures due to non-random cleavage of cell-free DNA. BMC Med. Genomics *8*, 29. https://doi.org/10.1186/s12920-015-0107-z.

23. Sanchez, C., Roch, B., Mazard, T., Blache, P., Dache, Z.A.A., Pastor, B., Pisareva, E., Tanos, R., and Thierry, A.R. (2021). Circulating nuclear DNA structural features, origins, and complete size profile revealed by fragmentomics. JCI Insight *6*, e144561. https://doi.org/10.1172/jci.insight.144561.

24. Marimuthu, A., O'Meally, R.N., Chaerkady, R., Subbannayya, Y., Nanjappa, V., Kumar, P., Kelkar, D.S., Pinto, S.M., Sharma, R., Renuse, S., et al. (2011). A comprehensive map of the human urinary proteome. J. Proteome Res. *10*, 2734–2743. https://doi.org/10.1021/pr2003038.

25. Hu, Z., Chen, H., Long, Y., Li, P., and Gu, Y. (2021). The main sources of circulating cell-free DNA: Apoptosis, necrosis and active secretion. Crit. Rev. Oncol. Hematol. *157*, 103166. https://doi.org/10.1016/j.critrevonc.2020.103166.

26. Hall, J.E. (2020). Guyton and Hall Textbook of Medical Physiology (Elsevier).

27. Haraldsson, B., Nyström, J., and Deen, W.M. (2008). Properties of the glomerular barrier and mechanisms of proteinuria. Physiol. Rev. *88*, 451–487. https://doi.org/10.1152/physrev.00055.2006.

28. Jia, L., Zhang, L., Shao, C., Song, E., Sun, W., Li, M., and Gao, Y. (2009). An Attempt to Understand Kidney's Protein Handling Function by Comparing Plasma and Urine Proteomes. PLoS One *4*, e5146. https://doi.org/10.1371/journal.pone.0005146.

29. Mayanagi, K., Saikusa, K., Miyazaki, N., Akashi, S., Iwasaki, K., Nishimura, Y., Morikawa, K., and Tsunaka, Y. (2019). Structural visualization of key steps in nucleosome reorganization by human FACT. Sci. Rep. *9*, 10183. https://doi.org/10.1038/s41598-019-46617-7.

30. Li, B., Carey, M., and Workman, J.L. (2007). The Role of Chromatin during Transcription. Cell *128*, 707–719. https://doi.org/10.1016/j.cell.2007.01.015.

31. Venkatesh, S., and Workman, J.L. (2015). Histone exchange, chromatin structure and the regulation of transcription. Nat. Rev. Mol. Cell. Biol. *16*, 178–189. https://doi.org/10.1038/nrm3941.

32. Berger, S.L. (2007). The complex language of chromatin regulation during transcription. Nature *447*, 407–412. https://doi.org/10.1038/nature05915.

33. Li, E. (2002). Chromatin modification and epigenetic reprogramming in mammalian development. Nat. Rev. Genet. *3*, 662–673. https://doi.org/10.1038/nrg887.

34. Wenger, A., Biran, A., Alcaraz, N., Redó-Riveiro, A., Sell, A.C., Krautz, R., Flury, V., Reverón-Gómez, N., Solis-Mezarino, V., Völker-Albert, M., et al. (2023). Symmetric inheritance of parental histones governs epigenome maintenance and embryonic stem cell identity. Nat. Genet. *55*, 1567–1578. https://doi.org/10.1038/s41588-023-01476-x.

35. Bannister, A.J., and Kouzarides, T. (2011). Regulation of chromatin by histone modifications. Cell Res. *21*, 381–395. https://doi.org/10.1038/cr.2011.22.

36. Wang, M., Yu, Q., Wang, L., and Gu, H. (2013). Distinct patterns of histone modifications at cardiac-specific gene promoters between cardiac stem cells and mesenchymal stem cells. Am. J. Physiol. Cell Physiol. *304*, C1080–C1090. https://doi.org/10.1152/ajpcell.00359.2012.

37. Krivtsov, A.V., and Armstrong, S.A. (2007). MLL translocations, histone modifications and leukaemia stem-cell development. Nat. Rev. Cancer *7*, 823–833. https://doi.org/10.1038/nrc2253.

38. Chervona, Y., and Costa, M. (2012). Histone modifications and cancer: biomarkers of prognosis? Am. J. Cancer Res. *2*, 589–597.

39. Audia, J.E., and Campbell, R.M. (2016). Histone Modifications and Cancer. Cold Spring Harb. Perspect. Biol. *8*, a019521. https://doi.org/10.1101/cshperspect.a019521.

40. Vad-Nielsen, J., Meldgaard, P., Sorensen, B.S., and Nielsen, A.L. (2020). Cell-free Chromatin Immunoprecipitation (cfChIP) from blood plasma can determine gene-expression in tumors from non-small-cell lung cancer patients. Lung Cancer *147*, 244–251. https://doi.org/10.1016/j.lungcan.2020.07.023.

41. Trier Maansson, C., Meldgaard, P., Stougaard, M., Nielsen, A.L., and Sorensen, B.S. (2023). Cell-free chromatin immunoprecipitation can determine tumor gene expression in lung cancer patients. Mol. Oncol. *17*, 722–736. https://doi.org/10.1002/1878-0261.13394.

42. Sadeh, R., Sharkia, I., Fialkoff, G., Rahat, A., Gutin, J., Chappleboim, A., Nitzan, M., Fox-Fisher, I., Neiman, D., Meler, G., et al. (2021). ChIP-seq of plasma cell-free nucleosomes identifies gene expression programs of the cells of origin. Nat. Biotechnol. *39*, 586–598. https://doi.org/10.1038/s41587-020-00775-6.

43. Barrero, M.J., Boué, S., and Izpisúa Belmonte, J.C. (2010). Epigenetic mechanisms that regulate cell identity. Cell Stem Cell *7*, 565–570. https://doi.org/10.1016/j.stem.2010.10.009.

44. Richters, A., Aben, K.K.H., and Kiemeney, L.A.L.M. (2020). The global burden of urinary bladder cancer: an update. World J. Urol. *38*, 1895–1904. https://doi.org/10.1007/s00345-019-02984-4.

45. Babjuk, M., Burger, M., Capoun, O., Cohen, D., Compérat, E.M., Dominguez Escrig, J.L., Gontero, P., Liedberg, F., Masson-Lecomte, A., Mostafid, A.H., et al. (2022). European Association of Urology Guidelines on Non-muscle-invasive Bladder Cancer (Ta, T1, and Carcinoma in Situ). Eur. Urol. *81*, 75–94. https://doi.org/10.1016/j.eururo.2021.08.010.

46. Sylvester, R.J., van der Meijden, A.P.M., Oosterlinck, W., Witjes, J.A., Bouffioux, C., Denis, L., Newling, D.W.W., and Kurth, K. (2006). Predicting recurrence and progression in individual patients with stage Ta T1 bladder cancer using EORTC risk tables: a combined analysis of 2596 patients from seven EORTC trials. Eur. Urol. *49*, 466–477, discussion 475–477. https://doi.org/10.1016/j.eururo.2005.12.031.

47. Golla, V., and Chamie, K. (2021). Oncological Monitoring of NonMuscle Invasive Bladder Cancer (NMIBC). In Bladder Cancer, pp. 123–138. https://doi.org/10.1007/978-3-030-70646-3_13.

48. Stav, K., Leibovici, D., Goren, E., Livshitz, A., Siegel, Y.I., Lindner, A., and Zisman, A. (2004). Adverse effects of cystoscopy and its impact on patients' quality of life and sexual performance. Isr. Med. Assoc. J. *6*, 474–478.

49. Kundaje, A., Meuleman, W., Ernst, J., Bilenky, M., Yen, A., Heravi-Moussavi, A., Kheradpour, P., Zhang, Z., Wang, J., et al.; Roadmap Epigenomics Consortium (2015). Integrative analysis of 111 reference human epigenomes. Nature *518*, 317–330. https://doi.org/10.1038/nature14248.

50. Ernst, J., and Kellis, M. (2017). Chromatin-state discovery and genome annotation with ChromHMM. Nat. Protoc. *12*, 2478–2492. https://doi.org/10.1038/nprot.2017.124.

51. Wood, A., and Shilatifard, A. (2004). Posttranslational Modifications of Histones by Methylation. Adv. Protein Chem. *67*, 201–222. https://doi.org/10.1016/S0065-3233(04)67008-2.

52. van der Pol, Y., Tantyo, N.A., Evander, N., Hentschel, A.E., Wever, B.M., Ramaker, J., Bootsma, S., Fransen, M.F., Lenos, K.J., Vermeulen, L., et al. (2023). Real-time analysis of the cancer genome and fragmentome from plasma and urine cell-free DNA using nanopore sequencing. EMBO Mol. Med. *15*, e17282. https://doi.org/10.15252/emmm.202217282.

53. Bryzgunova, O.E., Skvortsova, T.E., Kolesnikova, E.V., Starikov, A.V., Rykova, E.Y., Vlassov, V.V., and Laktionov, P.P. (2006). Isolation and comparative study of cell-free nucleic acids from human urine. Ann. N.Y. Acad. Sci. *1075*, 334–340. https://doi.org/10.1196/annals.1368.045.

54. Markus, H., Zhao, J., Contente-Cuomo, T., Stephens, M.D., Raupach, E., Odenheimer-Bergman, A., Connor, S., McDonald, B.R., Moore, B., Hutchins, E., et al. (2021). Analysis of recurrently protected genomic regions in cell-free DNA found in urine. Sci. Transl. Med. *13*, eaaz3088. https://doi.org/10.1126/scitranslmed.aaz3088.

55. Cherepanova, A., Tamkovich, S., Pyshnyi, D., Kharkova, M., Vlassov, V., and Laktionov, P. (2007). Immunochemical assay for deoxyribonuclease activity in body fluids. J. Immunol. Methods *325*, 96–103. https://doi.org/10.1016/j.jim.2007.06.004.

56. Nadano, D., Yasuda, T., and Kishi, K. (1993). Measurement of deoxyribonuclease I activity in human tissues and body fluids by a single radial enzyme-diffusion method. Clin. Chem. *39*, 448–452. https://doi.org/10.1093/clinchem/39.3.448.

57. Furuyama, T., Codomo, C.A., and Henikoff, S. (2013). Reconstitution of hemisomes on budding yeast centromeric DNA. Nucleic Acids Res. *41*, 5769–5783. https://doi.org/10.1093/nar/gkt314.

58. Kueng, N., Sidler, D., Banz, V., Largiadèr, C.R., Ng, C.K.Y., and Amstutz, U. (2023). Investigation of Different Library Preparation and Tissue of Origin Deconvolution Methods for Urine and Plasma cfDNA Methylome Analysis. Diagnostics *13*, 2505. https://doi.org/10.3390/diagnostics13152505.

59. Cheng, A.P., Burnham, P., Lee, J.R., Cheng, M.P., Suthanthiran, M., Dadhania, D., and De Vlaminck, I. (2019). A cell-free DNA metagenomic sequencing assay that integrates the host injury response to infection. Proc. Natl. Acad. Sci. USA *116*, 18738–18744. https://doi.org/10.1073/pnas.1906320116.

60. Wang, Y., Zhao, Y., Zhao, Z., Li, D., Nie, H., Sun, Y., Feng, X., Zhang, T., Ma, Y., Nie, J., et al. (2021). Single-cell RNA-Seq analysis identified kidney progenitor cells from human urine. Protein Cell *12*, 305–312. https://doi.org/10.1007/s13238-020-00816-5.

61. Abedini, A., Zhu, Y.O., Chatterjee, S., Halasz, G., Devalaraja-Narashimha, K., Shrestha, R., S Balzer, M., Park, J., Zhou, T., Ma, Z., et al. (2021). Urinary Single-Cell Profiling Captures the Cellular Diversity of the Kidney. J. Am. Soc. Nephrol. *32*, 614–627. https://doi.org/10.1681/ASN.2020050757.

62. Belik, R., Follmann, W., Degen, G.H., Roos, P.H., Blaszkewicz, M., Knopf, H.J., and Golka, K. (2008). Improvements in culturing exfoliated urothelial cells in vitro from human urine. J. Toxicol. Environ. Health. A *71*, 923–929. https://doi.org/10.1080/15287390801988871.

63. Kunin, C.M., Evans, C., Bartholomew, D., and Bates, D.G. (2002). The antimicrobial defense mechanism of the female urethra: a reassessment. J. Urol. *168*, 413–419.

64. Wu, H.H.L., Goldys, E.M., Pollock, C.A., and Saad, S. (2022). Exfoliated Kidney Cells from Urine for Early Diagnosis and Prognostication of CKD: The Way of the Future? Int. J. Mol. Sci. *23*, 7610. https://doi.org/10.3390/ijms23147610.

65. Moss, J., Magenheim, J., Neiman, D., Zemmour, H., Loyfer, N., Korach, A., Samet, Y., Maoz, M., Druid, H., Arner, P., et al. (2018). Comprehensive human cell-type methylation atlas reveals origins of circulating cell-free DNA in health and disease. Nat. Commun. *9*, 5068. https://doi.org/10.1038/s41467-018-07466-6.

66. Moss, J., Ben-Ami, R., Shai, E., Gal-Rosenberg, O., Kalish, Y., Klochendler, A., Cann, G., Glaser, B., Arad, A., Shemer, R., and Dor, Y. (2023). Megakaryocyte- and erythroblast-specific cell-free DNA patterns in plasma and platelets reflect thrombopoiesis and erythropoiesis levels. Nat. Commun. *14*, 7542. https://doi.org/10.1038/s41467-023-43310-2.

67. Shekhtman, E.M., Anne, K., Melkonyan, H.S., Robbins, D.J., Warsof, S.L., and Umansky, S.R. (2009). Optimization of transrenal DNA analysis: detection of fetal DNA in maternal urine. Clin. Chem. *55*, 723–729. https://doi.org/10.1373/clinchem.2008.113050.

68. Majer, S., Bauer, M., Magnet, E., Strele, A., Giegerl, E., Eder, M., Lang, U., and Pertl, B. (2007). Maternal urine for prenatal diagnosis–an analysis of cell-free fetal DNA in maternal urine and plasma in the third trimester. Prenat. Diagn. *27*, 1219–1223. https://doi.org/10.1002/pd.1875.

69. Breyer, J., Wirtz, R.M., Otto, W., Erben, P., Kriegmair, M.C., Stoehr, R., Eckstein, M., Eidt, S., Denzinger, S., Burger, M., et al. (2017). In stage pT1 non-muscle-invasive bladder cancer (NMIBC), high KRT20 and low KRT5 mRNA expression identify the luminal subtype and predict recurrence and survival. Virchows Arch. *470*, 267–274. https://doi.org/10.1007/s00428-017-2064-8.

70. Wezel, F., Lustig, J., Azoitei, A., Liu, J., Meessen, S., Najjar, G., Zehe, V., Faustmann, P., Zengerling, F., John, A., et al. (2021). Grainyhead-Like 3

Influences Migration and Invasion of Urothelial Carcinoma Cells. Int. J. Mol. Sci. *22*, 2959. https://doi.org/10.3390/ijms22062959.

71. Hsu, Y.-P., Yang, H.-W., Li, N.-S., Chen, Y.-T., Pang, H.-H., and Pang, S.-T. (2020). Instrument-Free Detection of FXYD3 Using Vial-Based Immunosensor for Earlier and Faster Urothelial Carcinoma Diagnosis. ACS Sens. *5*, 928–935. https://doi.org/10.1021/acssensors.9b02013.
72. Turner, K.J., Crew, J.P., Wykoff, C.C., Watson, P.H., Poulsom, R., Pastorek, J., Ratcliffe, P.J., Cranston, D., and Harris, A.L. (2002). The hypoxia-inducible genes VEGF and CA9 are differentially regulated in superficial vs invasive bladder cancer. Br. J. Cancer *86*, 1276–1282. https://doi.org/10.1038/sj.bjc.6600215.
73. Wang, F.-H., Ma, X.-J., Xu, D., and Luo, J. (2018). UPK1B promotes the invasion and metastasis of bladder cancer via regulating the Wnt/β-catenin pathway. Eur. Rev. Med. Pharmacol. Sci. *22*, 5471–5480. https://doi.org/10.26355/eurrev_201809_15807.
74. Kuleshov, M.V., Jones, M.R., Rouillard, A.D., Fernandez, N.F., Duan, Q., Wang, Z., Koplev, S., Jenkins, S.L., Jagodnik, K.M., Lachmann, A., et al. (2016). Enrichr: a comprehensive gene set enrichment analysis web server 2016 update. Nucleic Acids Res. *44*, W90–W97. https://doi.org/10.1093/nar/gkw377.
75. Lachmann, A., Torre, D., Keenan, A.B., Jagodnik, K.M., Lee, H.J., Wang, L., Silverstein, M.C., and Ma'ayan, A. (2018). Massive mining of publicly available RNA-seq data from human and mouse. Nat. Commun. *9*, 1366. https://doi.org/10.1038/s41467-018-03751-6.
76. Mengus, C., Schultz-Thater, E., Coulot, J., Kastelan, Z., Goluza, E., Coric, M., Spagnoli, G.C., and Hudolin, T. (2013). MAGE-A10 cancer/testis antigen is highly expressed in high-grade non-muscle-invasive bladder carcinomas. Int. J. Cancer *132*, 2459–2463. https://doi.org/10.1002/ijc.27914.
77. Streleckiene, G., Reid, H.M., Arnold, N., Bauerschlag, D., and Forster, M. (2018). Quantifying cell free DNA in urine: comparison between commercial kits, impact of gender and inter-individual variation. Biotechniques *64*, 225–230. https://doi.org/10.2144/btn-2018-0003.
78. (2003). Pathophysiology of proteinuria. Kidney Int. *63*, 809–825. https://doi.org/10.1046/j.1523-1755.2003.00840.x.
79. Dermody, S.M., Bhambhani, C., Swiecicki, P.L., Brenner, J.C., and Tewari, M. (2022). Trans-Renal Cell-Free Tumor DNA for Urine-Based Liquid Biopsy of Cancer. Front. Genet. *13*, 879108. https://doi.org/10.3389/fgene.2022.879108.
80. Yu, S.C.Y., Deng, J., Qiao, R., Cheng, S.H., Peng, W., Lau, S.L., Choy, L.Y.L., Leung, T.Y., Wong, J., Wong, V.W.-S., et al. (2023). Comparison of Single Molecule, Real-Time Sequencing and Nanopore Sequencing for Analysis of the Size, End-Motif, and Tissue-of-Origin of Long Cell-Free DNA in Plasma. Clin. Chem. *69*, 168–179. https://doi.org/10.1093/clinchem/hvac180.
81. Rumore, P.M., and Steinman, C.R. (1990). Endogenous circulating DNA in systemic lupus erythematosus. Occurrence as multimeric complexes bound to histone. J. Clin. Investig. *86*, 69–74. https://doi.org/10.1172/JCI114716.
82. Gauthier, V.J., Tyler, L.N., and Mannik, M. (1996). Blood clearance kinetics and liver uptake of mononucleosomes in mice. J. Immunol. *156*, 1151–1156.
83. Uhlén, M., Fagerberg, L., Hallström, B.M., Lindskog, C., Oksvold, P., Mardinoglu, A., Sivertsson, Å., Kampf, C., Sjöstedt, E., Asplund, A., et al. (2015). Proteomics. Tissue-based map of the human proteome. Science *347*, 1260419. https://doi.org/10.1126/science.1260419.
84. Rasti, A., Khalili, M., Fakhr Yasseri, A.M., Nasirian, N., Shirkoohi, R., Nowroozi, M.R., and Modarressi, M.H. (2023). Evaluation of IGF2, KRT14, and KRT20 as Urinary Biomarkers in Patients with Bladder Cancer. Rep. Biochem. Mol. Biol. *11*, 710–719. https://doi.org/10.52547/rbmb.11.4.710.
85. Lokeshwar, V.B., Morera, D.S., Hasanali, S.L., Yates, T.J., Hupe, M.C., Knapp, J., Lokeshwar, S.D., Wang, J., Hennig, M.J.P., Baskar, R., et al. (2020). A Novel Splice Variant of HYAL-4 Drives Malignant Transformation and Predicts Outcome in Patients with Bladder Cancer. Clin. Cancer Res. *26*, 3455–3467. https://doi.org/10.1158/1078-0432.CCR-19-2912.
86. Salas, L.A., Wiencke, J.K., Koestler, D.C., Zhang, Z., Christensen, B.C., and Kelsey, K.T. (2018). Tracing human stem cell lineage during development using DNA methylation. Genome Res. *28*, 1285–1295. https://doi.org/10.1101/gr.233213.117.
87. Thierry, A.R. (2023). Circulating DNA fragmentomics and cancer screening. Cell Genom. *3*, 100242. https://doi.org/10.1016/j.xgen.2022.100242.
88. Sorber, L., Zwaenepoel, K., Jacobs, J., De Winne, K., Van Casteren, K., Augustus, E., Lardon, F., Prenen, H., Peeters, M., Van Meerbeeck, J., et al. (2020). Specialized Blood Collection Tubes for Liquid Biopsy: Improving the Pre-analytical Conditions. Mol. Diagn. Ther. *24*, 113–124. https://doi.org/10.1007/s40291-019-00442-w.
89. Langmead, B., and Salzberg, S.L. (2012). Fast gapped-read alignment with Bowtie 2. Nat. Methods *9*, 357–359. https://doi.org/10.1038/nmeth.1923.
90. Li, H., Handsaker, B., Wysoker, A., Fennell, T., Ruan, J., Homer, N., Marth, G., Abecasis, G., and Durbin, R.; 1000 Genome Project Data Processing Subgroup (2009). The Sequence Alignment/Map format and SAMtools. Bioinformatics *25*, 2078–2079. https://doi.org/10.1093/bioinformatics/btp352.

## STAR★METHODS

### KEY RESOURCES TABLE

| REAGENT or RESOURCE | SOURCE | IDENTIFIER |
|---|---|---|
| Critical commercial assays | | |
| Senseera cfChIP-seq kit | https://www.senseerahealth.com/ | |
| Zymo cfDNA extraction kit | Zymo Research | ZR-R1072 |
| Chemicals, peptides, and recombinant proteins | | |
| protease inhibitors | Roche | 5056489001 |
| Micrococcal nuclease | Worthington Biochemical | LS004798 |
| Bovine Serum Heat inactivated | Rockland | D500-05-0500 |
| Software and algorithms | | |
| cfChIP-seq analysis | Sadeh et al.[42] | https://github.com/nirfriedman/cfChIP-seq; https://doi.org/10.5281/zenodo.15766044 |
| cfChIP-seq urine specific setup files | This study | https://doi.org/10.5281/zenodo.3967253 |
| bowtie2 (2.4.2) | Langmead et al., 2012[89] | https://bowtie-bio.sourceforge.net/bowtie2/index.shtml |
| samtools (1.7) | Li et al., 2009[90] | https://www.htslib.org/ |
| R programming language (4.0.2) | | https://www.r-project.org/ |
| Deposited data | | |
| cfChiP-seq data | This study | https://doi.org/10.5281/zenodo.15227938 |
| Raw and analyzed ChIP-seq | ENCODE3 project | https://www.encodeproject.org/ |
| Raw and analyzed ChIP-seq | BLUEPRINT project | https://epigenomesportal.ca/ihec/ |

### EXPERIMENTAL MODEL AND STUDY PARTICIPANT DETAILS

#### Donors

The relevant local ethics committees approved all clinical studies. The study was approved by the Institutional Review Boards (IRBs) of the Hadassah-Hebrew University Medical Center of Jerusalem and the Hebrew University. Informed consent was obtained from all individuals before blood and urine sampling.

### METHOD DETAILS

#### Sample collection

~20 mL urine samples were collected in standard plastic collection cups supplemented with EDTA to a final concentration for 10mM to prevent DNase digestion. Samples were transferred to conical 50mL tubes and centrifuged immediately at room temperature at a speed of 3000g for 10 min. The urine supernatant was transferred to a second 50 mL conical tube while being careful not to disturb any cell debris. The urine supernatant was centrifuged and transferred again using the same settings as before to ensure no cellular debris. The doubly centrifuged urine was used for the cfChIP-seq experiments. Urine cfChIP-seq was performed immediately or after storage at 4C for at most 2 weeks, per our preanalytic experiment results (Figure S7).

Plasma samples were collected as described in Sadeh et al. 2021.[42] Briefly, Blood samples were collected in VACUETTE K3 EDTA tubes and transferred to ice. The blood was centrifuged (10 min, 1,500g, 4°C) and the supernatant was transferred to a fresh 15-mL tube and centrifuged again (10 min, 3,000g, 4°C). The supernatant plasma was used for ChIP experiments. The plasma was used fresh or flash-frozen and stored at −80°C for long-term storage.

#### H3K4me3 ChIP-seq of urine-exfoliated cells

Urine samples were collected as above except for urine-exfoliated cells collection after initial centrifugation. After moving urine to a fresh tube, pelleted cells were washed using ice-cold 1X PBS supplemented with protease inhibitors (Roche cat. 5056489001). Cells were counted [Bio-Rad TC20 Cell Counter] and resuspended using supplemented NP buffer [10 mM Tris pH 7.4, 50 mM NaCl, 5 mM MgCl2, 1 mM CaCl2, and 0.075% NP-40, supplemented with fresh 1 mM β-mercaptoethanol, 500 μM spermidine]. Chromatin was digested with Micrococcal nuclease [Worthington Biochemical LS004798] at 5 units per 1 million cells. Chromatin was collected by centrifugation (14,000xg, 10 min at 4C) and quantified (Qubit 4 Fluorometer, Agilent TapeStation). Native H3K4me3 ChIP-seq was

performed in 500ul SDSless RIPA [10 mM Tris pH 8.0, 140 mM NaCl, 1 mM EDTA, 1% Triton X-100] or Bovine Serum Heat inactivated (Rockland D500-05-0500) using the same protocol as for urine cfChIP-seq.

### Urine cfDNA extraction

cfDNA from urine samples (collected as above) was extracted using Zymo cfDNA extraction kit [Zymo Research ZR-R1072] according to manufacturer's instructions.

### Immunoprecipitation, NGS library preparation, and sequencing

Immunoprecipitation, library preparation, and sequencing were performed by Senseera LTD as previously reported in Sadeh et al.[42] with slight modifications. Briefly, ChIP antibodies were covalently immobilized to paramagnetic beads and incubated with urine at room temperature overnight or plasma at 4C overnight. For paired-end Illumina sequencing using the NextSeq 550 platform, barcoded sequencing adaptors were ligated to chromatin fragments, and DNA was isolated according to the manufacturer's protocol.

### Sequencing analysis

Paired-end reads were processed by demultiplexing and aligned to the human genome (hg19) using bowtie2[89] (2.4.2) with 'no-mixed' and 'no-discordant' flags. Fragments with low alignment scores (flag -q 2). Duplicate fragments were discarded. See Table S1 for total number of reads, alignment statistics, and number of unique fragments for each sample. BAM files were processed by samtools[90] (1.7) to BED files and by R (4.0.2) scripts (see 'Code availability').

Preprocessing of sequencing data was performed as previously described in Sadeh et al.[42] Briefly, we constructed a TSS catalog using genomic annotations from ChromHMM, Roadmap Epigenomics, ENSEMBL and UCSC Genome Browser gene annotations. The human genome was segmented into discrete windows representing gene TSS and background. The sequenced reads covering each region were summed with non-specific reads estimated per sample and then subtracted, resulting in the specific signal in every window. Signal -counts were normalized and scaled to 1 million reads in healthy reference, accounting for sequencing depth differences. Detailed information regarding these steps can be found at the Supplementary Note in Sadeh et al.[42]

### Epigenomics atlas

We downloaded 414 samples of H3K4me3 ChIP-seq aligned read data from the ENCODE Epigenomics consortium (https://www.encodeproject.org/) and BLUEPRINT database (https://epigenomesportal.ca/ihec/). BAM files aligned to the hg19 human genome version were processed into BED format precisely as described above. Hg38 aligned BAM files were converted into hg19 and then processed as above.

Table S4 lists all cell types used as reference data. The BED files were then processed using the same scripts as cfChIP-seq samples.

### Tissue signatures

Using the ENCODE and Roadmap Epigenomics metadata tables, we defined sets of samples that belong to a tissue or group of tissues (see Table S4). We then defined the set of specific windows for each group of samples as meeting the following criteria: 1. The window is not predefined as a background region in the genome. 2. The window is not located on the Y chromosome. 3. A window must have at least two samples within the group satisfy the condition that they have >10 normalized reads, and <5 in all other samples outside the group, or >30 normalized reads and <10 in all other samples - the last condition allows minimal signal from contaminating populations such as immune-populations in solid tissues. Groups for which we found less than 20 specific windows were considered without a signature. The signature-scores are defined as the sum of normalized reads across signature windows divided by window lengths (normalized reads/kb).

### Tissue sources of cancer upregulated genes

Genes found to have a significantly increased signal in the NMIBC cohort, with a 2-fold increase in signal within a single tissue or cell type, were classified together (Figures 4D and S5E). Of 177 genes, 19 were increased only in macrophages/monocytes, and were classified as phagocytes due to their similarity. 22 were classified as T-cells. 122 genes had an increased signal in multiple solid tissues with no clear distinction. 15 genes had low (less than five normalised reads) in all tissues within the atlas, representing either rare cell types or abnormal gene regulation.

### Cancer-signature

Genes with significantly increased signal in the NMIBC cohort samples were filtered for those with a maximum of 3 normalized reads in healthy samples. This set of 43 genes was termed cancer-signature (Table S3).

## QUANTIFICATION AND STATISTICAL ANALYSIS

All custom statistical analyses are thoroughly described in Sadeh et al.[42] and briefly described below (Figures 4E and 4F). Computed *p*-values were corrected for multiple hypotheses using FDR and estimated as q values (R function p.adjust()).

### Comparison to background

We test whether the total sum of reads over a collection of windows (a signature, gene promoter windows, etc.) is larger than we would expect from the background signal (Figure 2B). The null hypothesis is that the number of reads in the windows of interest is Poisson distributed according to the estimated background rate at these windows.

### Comparison to healthy reference

We test whether the total sum of reads over a collection of windows is higher than we would expect according to the mean and variance in healthy donor reference samples (either in plasma or in urine references) with additional Poisson sampling variation[42] (Figures 4A and S5B).

### Comparison of two groups of samples

For each gene in each group, mean and variance were estimated under a model distribution (Figures 4B and S5C). We use a likelihood ratio test (LRT) where, under the null hypothesis, the statistic's distribution is approximately a Chi-squared distribution with 2 degrees of freedom, allowing us to compute the *p*-value.

### ROC analysis based on cancer signature scores

We assessed the performance of a cancer signature by computing a score for each sample, defined as the sum of normalized cfChIP-seq signal values across signature genes (Figure 4E). We used leave-one-out cross-validation (LOOCV) within the discovery dataset to evaluate performance. Discriminative ability was measured by the area under the ROC curve (AUC), with confidence intervals estimated using DeLong's method via the pROC R package. An independent, held-out validation cohort of 23 healthy subjects and 12 NMIBC patients urine samples withheld from analysis, was used to confirm the signature's generalizability, applying the same scoring approach and calculating the corresponding ROC AUC.